Airborne maritime target tracking by using magnetic anomaly detection signature

Rajiv Sithiravel, Bhashyam Balaji, Bradley Nelson, Ratnasingham Tharmarasa and Thiagalingam Kirubarajan

***Abstract*—For an airborne sensor there is a pressing need to be able to detect/track submerged submarines, shipwrecks, sea-mines, unexploded explosive ordnance (UXO) and buried drums during maritime surveillance. Traditional usage is the magnetic anomaly detection (MAD), where the small changes in the Earth's magnetic field caused by the ferrous components of the targets are measured. The primary means of long-range detection and classification of targets are with passive and active acoustic sensors, and MAD is used for accurate final localization. It could also be used for land-based targets but this is not common. Knowing the relationship between the magnetic signature and the kinematic parameters, the tracking problem can be formulated under a Bayesian framework. In this paper, an Extended Kalman filter (EKF), Generic Particle filter (GPF), Auxiliary Particle filter (APF) and a combination of Extended Kalman filter and Generic Particle filter (EKF-GPF) are used for a real single surface-target tracking problem in maritime surveillance using an airborne total-filed sensor. Given the total field measurements these filters are able to estimate the kinematic states as well as the permanent moments and induced moments effectively. Results are demonstrated the effectiveness of filters as well as the impact of using MAD as part of an airborne sensor.**

***Index Terms*—Maritime surveillance, Magnetic anomaly detection, Nonlinear target tracking, Particle filters, Extended Kalman filter, Airborne target tracking.**

I. Introduction

The magnetic anomaly detection (MAD) is the measure of any small changes in the Earth's magnetic field caused by any external disturbance [16, 17]. For example since a naval vessel contains ferromagnetic material, it becomes magnetized in the presence of the ambient Earth's magnetic field. The strength of this magnetic field can be measured by transiting past sea-floor/airborne magnetometers that measure the variation of the magnetic field components as a function of time. These variations are known as the magnetic signature of the vessels and it has two parts: induced and remanent (permanent) [4, 5].

Typically MAD can be applied in many areas including in search and warning. In military and civilian applications MAD is used as a search tool for submarine, shipwreck, mine, unexploded explosive ordnance (UXO) and buried drums detections [1, 14, 20, 22, 30]. Also MAD can predict warning and can facilitate the operation smoothly i.e., intruder detection (virtual fence, facilities protection, perimeter protection), access control (passage access control, entry points monitoring), medical application, industrial control and Geophysics. MAD data processing approaches include target based and noise based techniques [8, 9, 15, 23].

In maritime surveillance the magnetic signature of Navy vessels is of particular importance because sea mines use the magnetic signal as a trigger mechanism. The estimation of the magnetization is important because it allows one; I) to determine the currents of the degaussing coils to minimize the signature and/or II) to decide if the vessel requires a deperming operation. It has been shown in literature that using a combination of measured magnetic signatures and magnetic modeling quantitatively can predict the vessel permanent and induced magnetization [3, 4, 5, 7, 21, 26].

In Rapid Deployable System (RDS), array of acoustic and magnetic sensors are used for maritime surveillance. Once the data were collected and processed, the transmitted information would allow the detection, localization and classification of any vessel navigating in the area. The magnetic information was added to the acoustic information to decrease the probability of false alarm and to aid the classification of the ship. The non-acoustic methods, especially magnetic, for ships detection, tracking and classification have assumed greater importance in underwater applications where the acoustic methods give poor results, like in shallow waters, surf zones, and coastal regions [3, 6, 12, 29, 28]. When the vessel moves its magnetic signature as measured by a sensor varies with time. Of interest is the determination of the trajectory and magnetic parameters of the vessel from the magnetic signature measurements. Note, MAD has commonly not been considered as a sensor from which the data can be filtered from enhanced detection and tracking as is performed with data from the radar sensor. Further, its use in measuring the magnetic moment vector from targets has been limited to discrete fixes.

Previous works has indicated that the Kalman filtering [2] technique can estimate in real time the motion and magnetic parameters of a vessel modeled by an equivalent magnetic dipole [3, 6, 12, 29, 28]. In [3], the tracking problem is formulated in state-space form where the state variables are the position, velocity and magnetic moments of the target. The relationship between the magnetic measurements and the motion and magnetic parameters of the target is non-linear. Lately, several filtering algorithms became available for state estimation of non-linear systems. These filters are the EKF, two Kalman filters based on the Stirlings interpolation formula, and the unscented Kalman filter (UKF) [3, 6, 7, 8, 12, 29, 28]. They use various approximation of non-linear equation

R.Sithiravel and B.Balaji are with the Radar Sensing and Exploitation Section, Defence R&D Canada, Ottawa, ON, Canada. e-mail: Rajiv.Sithiravel@drdc-rddc.gc.ca and Bhashyam.Balaji@drdc-rddc.gc.ca

B. Nelson is the President of Aeromagnetic Solutions Incorporated, Ottawa, ON, Canada. e-mail: bnelson4640@rogers.com

R. Tharmarasa and T. Kirubarajan are with the Department of Electrical and Computer Engineering, McMaster University, Hamilton, ON, Canada. e-mail: tharman@mcmaster.ca and kiruba@mcmaster.ca

and thus their performances in solving the tracking problem will be different. The goal of this paper is to investigate the use of non-linear filters for the kinematic and magnetic dipole tracking applications, compare their performances and analyse the usefulness of MAD in sensor fusion.

The filters were exercised on a set of real data collected near the Bahamas using a total-field magnetic sensor (magnetometer), mounted in a National Research Council of Canada aircraft to record magnetic noise. Simulated target signatures from a single surface vessel with both permanent and induced magnetic dipole moments were then embedded in this noise. The estimation performance of the following non-linear filters are compared: the Extended Kalman filter (EKF), Generic Particle filter (GPF), Auxiliary Particle filter (APF) and a combination of Extended Kalman filter and Generic Particle filter (EKF-GPF) [2, 11]. The root mean square error (RMSE) [2], posterior Cramér-Rao lower bound (PCRLB) [25] and normalized estimation error squared (NEES) [2] are used as the performance evaluation criteria. As shown in the results, the best magnetic signal processor for this application is the particle filters. Using MAD based target tracking not only can the targets can be localized or/and tracked, but the magnetic parameters can be estimated. For friendly submarines, this information can be used to optimize the degaussing coil parameters to avoid both MAD detection and damage from sea mines. For friendly surface vessels, the information can be used to avoid damage from sea mines. In anti-submarine warfare, acoustic signals can be captured by using Cardioid sensors [10, 18]. Once initialized the target then MAD signatures can be used to track the target of interest. Therefore, inclusion of MAD as part of multi-sensor fusion can increase the efficiency of the target tracking as well as it usability [4].

The structure of this paper is as follows: Section II briefly review the system and measurement models. For further details of MAD theories readers can refer to [3], non-linear Bayesian filtering and the Posterior Cramér-Rao Lower Bound are explained in Sections III and IV, respectively. Sections V and VI are present the details derivation of Extended Kalman Filter and particle filters. In appendix, A pseudo-codes of particle filters along with resampling algorithm have been provided. Results and conclusions are given in Sections VII and VIII, respectively.

II. State and Measurement Models

The scenario deals with the maritime surveillance, where a single target with multidimensional state

$$\mathbf{x}(t) \quad = \quad [x_i(t)]_{i=1}^{n} \tag{1}$$

is assumed to be moving (a nearly constant velocity model for the kinematic portion) along the surface with zero altitude and n denotes the number of dimensions.

The target system evolves as

$$\mathbf{x}(t+1) \quad = \quad F\mathbf{x}(t) + \nu \tag{2}$$

where F and ν are denoted the system transition matrix and process noise vector, respectively. For general case (n=10) the target state conveys the kinematic, permanent magnetic moments and induced magnetic moments information. The system equation (2) can be re-written for general case as

$$\begin{bmatrix} \mathbf{x}_1(t_{k+1}) \\ \mathbf{x}_2(t_{k+1}) \\ \mathbf{x}_3(t_{k+1}) \\ \mathbf{x}_4(t_{k+1}) \\ \mathbf{x}_5(t_{k+1}) \\ \mathbf{x}_6(t_{k+1}) \\ \mathbf{x}_7(t_{k+1}) \\ \mathbf{x}_8(t_{k+1}) \\ \mathbf{x}_9(t_{k+1}) \\ \mathbf{x}_{10}(t_{k+1}) \end{bmatrix} = \begin{bmatrix} 1 & T & 0 & 0 & 0 & 0 & 0 & 0 & 0 & 0 \\ 0 & 1 & 0 & 0 & 0 & 0 & 0 & 0 & 0 & 0 \\ 0 & 0 & 1 & T & 0 & 0 & 0 & 0 & 0 & 0 \\ 0 & 0 & 0 & 1 & 0 & 0 & 0 & 0 & 0 & 0 \\ 0 & 0 & 0 & 0 & 1 & 0 & 0 & 0 & 0 & 0 \\ 0 & 0 & 0 & 0 & 0 & 1 & 0 & 0 & 0 & 0 \\ 0 & 0 & 0 & 0 & 0 & 0 & 1 & 0 & 0 & 0 \\ 0 & 0 & 0 & 0 & 0 & 0 & 0 & 1 & 0 & 0 \\ 0 & 0 & 0 & 0 & 0 & 0 & 0 & 0 & 1 & 0 \\ 0 & 0 & 0 & 0 & 0 & 0 & 0 & 0 & 0 & 1 \end{bmatrix} \cdot \begin{bmatrix} \mathbf{x}_1(t_k) \\ \mathbf{x}_2(t_k) \\ \mathbf{x}_3(t_k) \\ \mathbf{x}_4(t_k) \\ \mathbf{x}_5(t_k) \\ \mathbf{x}_6(t_k) \\ \mathbf{x}_7(t_k) \\ \mathbf{x}_8(t_k) \\ \mathbf{x}_9(t_k) \\ \mathbf{x}_{10}(t_k) \end{bmatrix} + \begin{bmatrix} \nu_1(t_k) \\ \nu_2(t_k) \\ \nu_3(t_k) \\ \nu_4(t_k) \\ \nu_5(t_k) \\ \nu_6(t_k) \\ \nu_7(t_k) \\ \nu_8(t_k) \\ \nu_9(t_k) \\ \nu_{10}(t_k) \end{bmatrix} \tag{3}$$

where

- ship's kinematic states are the 2-D position and velocity,position vector ($[x_1(t), x_3(t)]$) and velocity (or equivalently speed and heading) vector ($[x_2(t), x_4(t)]$),
- the permanent moments ($[x_5(t), x_6(t), x_7(t)] \equiv [M_{LP}, M_{TP}, M_{VP}]$,
- the induced moment parameters $[x_8(t), x_9(t), x_{10}(t)] \equiv [C_L W, C_T W, C_V W]$, and
- the sampling time T.

If the permanent and induced magnetic moments cannot be disentangled then (n=7) and system state does not have the induced moment information [3].

An airborne sensor is used to detect the target with probability of detection P_d. It is assumed that the sensor moves at a known constant altitude z_p, and the x- and y- position vectors ($[x_p(t), y_p(t)]$) and velocity (or equivalently speed and heading) vector ($[v_x(t), v_y(t)]$) are also assumed known.

The measurement model is

$$y(t_k) = \frac{1}{|\mathbf{B}_e|} \cdot \left(\frac{3(\mathbf{M}(t_k) \cdot \mathbf{R}(t_k))(\mathbf{R}(t_k) \cdot \mathbf{B}_e)}{|\mathbf{R}(t_k)|^5} - \frac{\mathbf{M}(t_k) \cdot \mathbf{B}_e}{|\mathbf{R}(t_k)|^3} \right) + \omega(t_k) \tag{4}$$

where $\omega(t_k)$ denotes the measurement noise, $\mathbf{R} \equiv [x_p(t) - x_1(t), y_p(t) - x_3(t), z_p]$ denotes the vector from the source dipole to the magnetometer (MAD sensor) in metres, $\mathbf{B}_e = [B_n, B_e, B_v]$ denotes the earth's magnetic field and $\mathbf{M}$ is the

total dipole moment vector (in nano Tesla meter^3) given as

$$\mathbf{M}(t) = \begin{bmatrix} \frac{x_2(t)}{\sqrt{x_2(t)^2+x_4(t)^2}} & \frac{x_4(t)}{\sqrt{x_2(t)^2+x_4(t)^2}} & 0 \\ -\frac{x_4(t)}{\sqrt{x_2(t)^2+x_4(t)^2}} & \frac{x_2(t)}{\sqrt{x_2(t)^2+x_4(t)^2}} & 0 \\ 0 & 0 & 1 \end{bmatrix} \times \left(\begin{bmatrix} x_5(t) \\ x_6(t) \\ x_7(t) \end{bmatrix} + \begin{bmatrix} x_8(t) \\ x_9(t) \\ x_{10}(t) \end{bmatrix} \odot \left\{ \begin{bmatrix} \frac{x_2(t)}{\sqrt{x_2(t)^2+x_4(t)^2}} & \frac{x_4(t)}{\sqrt{x_2(t)^2+x_4(t)^2}} & 0 \\ -\frac{x_4(t)}{\sqrt{x_2(t)^2+x_4(t)^2}} & \frac{x_2(t)}{\sqrt{x_2(t)^2+x_4(t)^2}} & 0 \\ 0 & 0 & 1 \end{bmatrix} \begin{bmatrix} B_r \\ B_e \\ B_v \end{bmatrix} \right\} \right) \quad (5)$$

(recalling that $\tan(\theta_s) = v_y/v_x = x_4(t)/x_2(t)$). If permanent and induced magnetic moments cannot be disentangled

$$\mathbf{M}(t) = \begin{bmatrix} \frac{x_2(t)}{\sqrt{x_2(t)^2+x_4(t)^2}} & \frac{x_4(t)}{\sqrt{x_2(t)^2+x_4(t)^2}} & 0 \\ -\frac{x_4(t)}{\sqrt{x_2(t)^2+x_4(t)^2}} & \frac{x_2(t)}{\sqrt{x_2(t)^2+x_4(t)^2}} & 0 \\ 0 & 0 & 1 \end{bmatrix} \cdot \left(\begin{bmatrix} x_5(t) \\ x_6(t) \\ x_7(t) \end{bmatrix} \right) \quad (6)$$

III. Nonlinear Bayesian Filtering

A single target system state evolves as

$$\mathbf{x}_k \quad = \quad f(\mathbf{x}_{k-1}, \nu_{k-1}) \qquad k \in \mathbb{N} \quad (7)$$

where $\mathbb{N}$, $\mathbf{x}_k = [x_k^i]_{i=1}^{n_x}$, $f(\cdot,\cdot)$ and ν are denoted the set of natural numbers, the state sequence with n_x dimensions, a possibly nonlinear function of states of $\mathbf{x}_{k-1}$ and process noise, respectively. The process noise is iid Gaussian with zero mean and known variance σ_ν^2. The objective of the tracking is to recursively estimate $\mathbf{x}_k$ from the measurements.

The measurement can be defined as

$$\mathbf{z}_k \quad = \quad h(\mathbf{x}_k, \varpi_k) \quad (8)$$

where $\mathbf{z}_k = [z_k^i]_{i=1}^{n_z}$, $h(\cdot,\cdot)$ and ϖ_k are denoted the observation with n_z dimensions, a nonlinear function and iid Gaussian measurement noise with zero mean and known variance σ_ϖ^2, respectively.

Suppose the prior density $p_{k-1|k-1}(\mathbf{x}_{k-1}|\mathbf{z}_{1:k-1})$ at time $k-1$ is available. Then using the Chapman-Kolmogorov equation the predicted density can be determined as

$$p_{k|k-1}(\mathbf{x}_k|\mathbf{z}_{1:k-1}) \quad = \quad \int p_{k|k-1}(\mathbf{x}_k|\mathbf{x}_{k-1}) \cdot p_{k-1|k-1}(\mathbf{x}_{k-1}|\mathbf{z}_{1:k-1}) \mu_s(d\mathbf{x}_{k-1}) \quad (9)$$

where $p_{k|k-1}(\mathbf{x}_k|\mathbf{x}_{k-1})$ denotes the Markov transition density. The set of all available measurements up to time $k-1$ is denoted by $\mathbf{z}_{1:k-1} = [\mathbf{z}_i]_{i=1}^{k-1}$.

The posterior pdf can be update with the available measurement at time k by using Bayes' rule as

$$p_{k|k}(\mathbf{x}_k|\mathbf{z}_{1:k}) \quad = \quad \frac{p_k(\mathbf{z}_k|\mathbf{x}_k) p_{k|k-1}(\mathbf{x}_k|\mathbf{z}_{1:k-1})}{\int p_k(\mathbf{z}_k|\mathbf{x}_k) p_{k|k-1}(\mathbf{x}_k|\mathbf{z}_{1:k-1}) \mu_s(d\mathbf{x}_k)} \quad (10)$$

where $p_{k|k-1}(\mathbf{x}_k|\mathbf{x}_{k-1})$ is the system model Markov transition density, $p_k(\mathbf{z}_k|\mathbf{x}_k)$ denotes the likelihood function and μ_s denotes an appropriate reference measure [27].

An optimal Bayesian solution can be determined using the recurrence relation (9) and (10), but the recursive propagation of the posterior density in general is only a conceptual. Note, it can not be determined analytically. If analytic solution is intractable, extended Kalman filter and particle filters can be used to approximate the optimal Bayesian solution.

IV. Posterior Cramér-Rao Lower Bound

A. Background

Assume a system and the measurement equations are given as (7) and (8). At time k let the unbiased estimates $\hat{\mathbf{x}}_k(\mathbf{z}_k)$ of $\mathbf{x}_k$ depend on the measurement data $\mathbf{z}_k$. The Posterior Cramér-Rao Lower Bound (PCRLB) is the inverse of the Fisher information matrix (FIM) $J(k)$. Using PCRLB can determine a lower bound of error covariance matrix, i.e.,

$$C(k) \triangleq \mathbb{E}\{[\hat{\mathbf{x}}_k(\mathbf{z}_k) - \mathbf{x}_k][\hat{\mathbf{x}}_k(\mathbf{z}_k) - \mathbf{x}_k]'\} \geqslant J(k)^{-1} \quad (11)$$

where $\mathbb{E}$ denotes the expectation and $C(k) - J(k)^{-1}$ is always positive semi-definite matrix.

Assume at time k the measured data is represented by $\mathbf{z}_k = [z_1, z_2, \ldots, z_k]$ and $\hat{\mathbf{x}}_k(\mathbf{z}_k)$ be an unbiased estimator of the r-dimensional vector $\mathbf{x}_k$ of random parameters. The PCRLB is defined to be the inverse, $J(k)^{-1}$, of the (in this case $r \times r$) Fisher Information Matrix (FIM), $J(k)$. This gives a lower bound on the error covariance of $\hat{\mathbf{x}}_k(\mathbf{z}_k)$:

$$C_k \triangleq \mathbb{E}\big\{[\hat{\mathbf{x}}_k(\mathbf{z}_k) - \mathbf{x}_k][\hat{\mathbf{x}}_k(\mathbf{z}_k) - \mathbf{x}_k]^T\big\} \geq J(k)^{-1} \quad (12)$$

where $\mathbb{E}$ denotes expectation over ($\mathbf{x}_k$, $\mathbf{z}_k$). The inequality in (12) means that $C_k - J(k)^{-1}$ is a positive semi-definite matrix.

B. PCRLB for a single target Tracking

Assume a target is moving with system state equation

$$\mathbf{x}_{k+1} \quad = \quad F_k \mathbf{x}_k + \nu_k \quad (13)$$

where F_k and ν_k are denoted a linear function and an independent white noise sequence, respectively.

The measurement $\mathbf{z}_k$ can originates from targets or noise. The target-originated ones detected with probability $P_d(k)$. The measurement at time index k

$$z_k^j = \begin{cases} h_k \mathbf{x}_k + \varpi_k & \text{if originated from target} \\ v_k^j & \text{if false alarm} \end{cases} \quad (14)$$

where z_k^j and h_k, ϖ_k are denoted the j-th measurement, a nonlinear function and a zero mean Gaussian random variable with covariance Σ_k, respectively. The number of false alarm in the sensor's field of view (FOV) is Poisson-distributed with mean λV and v_k^j is uniformly distributed throughout the FOV of the sensor. Note, λ is denoted false alarm rate.

Under the association assumption [2], in which each measurement must be associated with either one target or clutter, it can be shown that FIM, $J(k+1)$, is a block-diagonal matrix. Note, the initial FIM, given by $J(0) = C_0^{-1}$ is a block diagonal.

The FIM evolves during the recursion as

$$J(k+1) = \underbrace{\left[Q_k + F_k J(k)^{-1} (F_k)'\right]^{-1}}_{J_{\mathbf{x}}(k+1)} + J_{\mathbf{z}}(k+1) \quad (15)$$

where Q_k and $J_{\mathbf{z}}(k+1)$ are denoted the covariance of ν_k and the measurement information regarding target at time index $k+1$.

Under certain condition, $J_{\mathbf{z}}(k)$ is

$$J_{\mathbf{z}}(k) = \mathbb{E}\Big[q_k\big(H_k\big)^{'}\Sigma_k^{-1}H_k\Big] \tag{16}$$

and (a,b)-th element of matrix H_k is given by

$$H_k(a,b) = \frac{\partial h_k(a)}{\partial \mathbf{x}_k(b)} \tag{17}$$

where $h_k(a)$, $\mathbf{x}_k(b)$ are denoted the a-th component of the measurement vector and the b-th component of the state vector of target, respectively. The Information Reduction Factor (IRF) is denoted by q_k and it depends on the measurement noise covariance (Σ_k), false alarm rate (λ), probability of detection ($P_D(k)$) and the (gated) field of view (V) at time k. Note, the problem in this paper deals with a single target tracking without any false alarm. Since there is no measurement origin uncertainty $q_k = 1$.

V. Extended Kalman Filter

This section briefly describe the EKF and for more details refer to [2]. Using local linearization of system and measurement equations the EKF can reach a suboptimal solution for any given problem. The EKF often provide sufficient approximation of nonlinearity and densities are approximated using Gaussian. Lets consider a system evolves as (7) and the observations are taken as (8).

Assume prior density is available

$$p(\mathbf{x}_{k-1}|\mathbf{z}_{1:k-1}) \approx \mathcal{N}(\mathbf{x}_{k-1}; \mathbf{m}_{k-1|k-1}, P_{k-1|k-1}) \tag{18}$$

where $\mathcal{N}(\mathbf{x}_{k-1}; \mathbf{m}_{k-1|k-1}, P_{k-1|k-1})$ is a Gaussian density with argument $\mathbf{x}$, prior state mean $\mathbf{m}_{k-1|k-1}$ and prior state covariance $P_{k-1|k-1}$.

The state prediction density can be determined as

$$p(\mathbf{x}_k|\mathbf{z}_{1:k-1}) \approx \mathcal{N}(\mathbf{x}_k; \mathbf{m}_{k|k-1}, P_{k|k-1}) \tag{19}$$

where predicted state mean $\mathbf{m}_{k|k-1}$ can be determined using (7) as

$$\mathbf{m}_{k|k-1} = f(\mathbf{m}_{k-1|k-1}) \tag{20}$$

The predicted state covariance $P_{k|k-1}$ is

$$P_{k|k-1} = Q_{k-1} + \hat{F}_k P_{k-1|k-1}\hat{F}_k^{'} \tag{21}$$

where

$$\hat{F}_k = \frac{df_k(\mathbf{x})}{d\mathbf{x}}|_{\mathbf{x}=\mathbf{m}_{k-1|k-1}} \tag{22}$$

and the covariance matrix of the process noise $Q_{k-1} = \mathbb{E}[\nu_{k-1}\nu_{k-1}^{'}]$ where $\mathbb{E}$ denotes the expectation.

The filter gain can be determined as

$$W_k \quad = \quad P_{k|k-1}\hat{H}_k^{'}S_k^{-1} \tag{23}$$

where S_k denotes the residual covariance matrix that defined as

$$S_k \quad = \quad \hat{H}_k P_{k|k-1}\hat{H}_k^{'} + R_k, \tag{24}$$

using (8) h_k

$$\hat{H}_k = \frac{dh_k(\mathbf{x})}{d\mathbf{x}}|_{\mathbf{x}=\mathbf{m}_{k|k-1}} \tag{25}$$

can be determined and the covariance matrix of the measurement noise $R_k = \mathbb{E}[\varpi_k\varpi_k^{'}]$.

The posterior state mean and the state covariance at scan k can be determined as

$$\mathbf{m}_{k|k} \quad = \quad \mathbf{m}_{k|k-1} + W_k(\mathbf{z}_k - \hat{H}_k\mathbf{m}_{k|k-1}) \tag{26}$$

where $\mathbf{z}_k$ denotes the measurement at scan k and

$$P_{k|k} \quad = \quad P_{k|k-1} - W_k H_k P_{k|k-1} \tag{27}$$

The posterior density

$$p(\mathbf{x}_k|\mathbf{z}_{1:k}) \approx \mathcal{N}(\mathbf{x}_k; \mathbf{m}_{k|k}, P_{k|k}) \tag{28}$$

Using this recursive method a suboptimal solution to tracking problem can be achieved.

VI. Particle Filter

Particle filtering is a technique for implementing a recursive Bayesian filter by Monte Carlo (MC) simulations [11]. In here a required posterior density function is represented by a set of random samples with associated weights. The state estimates are computed based on these sample and weights. As the sample becomes larger the MC characterizations give the equivalent representation of posterior density function and the filter approaches the optimal solutions of state estimates.

Assume a tracking scenario with system (7) and measurement (8) models as in Section (III). The posterior density (10) $p(\mathbf{x}_{0:k}|\mathbf{z}_{1:k})$ can be characterised by random measures $\{\mathbf{x}_{0:k}^i, \omega_k^i\}_{i=1}^{N_s}$. Where $\mathbf{x}_{0:k}$ is the set of all states up to time k and $\{\mathbf{x}_{0:k}^i, i = 0, \cdots, N_s\}$ is a set of support points with associated weights $\{\omega_k^i, i = 1, \cdots, N_s\}$.

Then the posterior density at scan k can be approximated as

$$p(\mathbf{x}_{0:k}|\mathbf{z}_{1:k}) \approx \sum_{i=1}^{N_s} \omega_k^i \delta(\mathbf{x}_{0:k} - \mathbf{x}_{0:k}^i) \tag{29}$$

where δ denotes the delta function and the true posterior density have a discrete weighted approximation and $\sum_{i=1}^{N_s}\omega_k^i = 1$.

The weights are chosen using the principles of importance sampling (IS). The design of the importance sampling (IS) function critically affects the filtering performance [11] of the particle filter. One of the widely used methods is to approximate the IS function by the transition density [27]. Also, one can use the auxiliary particle approach to incorporate the measurement into the IS function as in the Auxiliary Particle filter (APF). Pseudo-code descriptions of regular, auxiliary particle filters are given in the appendix.

If the samples are drawn from important sampling density $q(\mathbf{x}_{0:k}|\mathbf{z}_{1:k})$ then the weights are defined as

$$\omega_k^i \propto \frac{p(\mathbf{x}_{0:k}|\mathbf{z}_{1:k})}{q(\mathbf{x}_{0:k}|\mathbf{z}_{1:k})} \tag{30}$$

For a common case when a filtered estimated is required (29) can be modified as

$$p(\mathbf{x}_k|\mathbf{z}_{1:k}) \approx \sum_{i=1}^{N_s} \omega_k^i \delta(\mathbf{x}_k - \mathbf{x}_k^i) \tag{31}$$

where as $N_s \rightarrow \infty$, the approximation (31) approaches the true posterior density $p(\mathbf{x}_k|\mathbf{z}_{1:k})$.

A. Degeneracy Problem

The degeneracy issue is a common problem for all the particle based filters. Generally, after few iterations, all but one particle will have a negligible weight. The variance of the important weights can only increase over time and therefore it is impossible to avoid the degeneracy problem. Also, in terms of complexity most of the time devoted to updated particle whose contribution to the approximation of $p(\mathbf{x}_k|\mathbf{z}_{1:k})$ is negligible. May use very large N_s to reduce the effect of the degeneracy, but often this is impractical for real problems. Method such as a) good choice of important density and b) resampling can be used to fix the degeneracy [11]. The resampling pseudo-code is explained in appendix.

B. EKF-GPF

In this algorithm EKF and GPF implementations are used. Initial particle $\mathbf{p}_{k-1}$ can be drawn from a known prior distribution and desire number of particles (N) at scan $k-1$. The initial weight ω_{k-1} vector's of each element value is selected to be $1/N$.

During the recursive particle and weight update, it is important to check to see it's time to resample or whether resampling is chosen already. If N is too few as result of resampling then rejuvenate i.e., draw a total of N samples with probabilities proportional to the weight vector ω, using residual resampling algorithm. The output rejuvenation vector's (outIndex) each element is an index into ω, or, the "parent" of the sample. Therefore if $\{\mathbf{x}, \omega\}$ is the original particles-weights pair, then $\{\mathbf{x}(\text{outIndex}), 1/N\}$ will be the sampled pair, where N is the total number of new particles, which can vary. Using outIndex, particles and weights are updated again. Note, it is important to internally keep track of when it's time to resample.

At scan k for each number of particles, weights ω_k and particles $\mathbf{p}_k(:,i)$ are updated as follows:

The prior mean is selected to be

$$\mathbf{m}_{k-1|k-1} = \mathbf{p}_{k-1}(:,i) \tag{32}$$

where i-th particle $\mathbf{p}$ is a vector.

The system state predicted mean is

$$\mathbf{m}_{k|k-1} = f(\mathbf{m}_{k-1|k-1}, T) \tag{33}$$

where f is a linear/nonlinear state equation and T denotes the sampling time.

The predicted measurement is

$$\mathbf{z}_{k|k-1} = h(\mathbf{m}_{k|k-1}, \mathbf{B}_e, \mathbf{S}_k) \tag{34}$$

where $\mathbf{B}_e = [B_n, B_e, B_v]$ and $\mathbf{S}_k = [x_p, y_p, z_p]$ are denoted as earth's magnetic field and sensor positions.

The jacobian of the nonlinear measurement function is needed for EKF and evaluated as

$$H_k = \frac{\partial h}{\partial \mathbf{x}}(\mathbf{x}, \mathbf{B}_e, \mathbf{S}_k)\,|_{\mathbf{x}=\mathbf{m}_{k|k-1}} \tag{35}$$

The system state covariance matrix is

$$\begin{aligned} P_k &= (Q_{k-1}^{-1} + H_k^{'} R_k^{-1} H_k)^{-1} \\ P_k &= (P_k + P_k^{'})/2 \end{aligned} \tag{36}$$

where Q_{k-1}, R_k are denoted as process and measurement noise covariance matrix. By adding P_k matrix and its transpose matrix then dividing by 2 can get a numerically asymmetric form of P_k matrix.

The mean of the state vector is updated as

$$\mathbf{m}_{k|k} = P_k(Q_{k-1}^{-1}\mathbf{m}_{k|k-1} + (H_k R_k^{-1}(\mathbf{z}_k - \mathbf{z}_{k|k-1} + H_k \mathbf{m}_{k|k-1}))^{'}) \tag{37}$$

where $\mathbf{z}_k$ denotes the current measurement.

Using the calculated P_k and $\mathbf{m}_{k|k}$ a Gaussian distribution is created and samples are drawn from the Gaussian distribution to propagate the particles $\mathbf{p}_k(:,i)$.

The transition density is determined using process model as

$$p(\mathbf{x}_k|\mathbf{x}_{k-1}) = \zeta_{\nu_d} \exp(-(\mathbf{p}_k(:,i) - \mathbf{m}_{k|k-1})' Q_{k-1}^{-1}(\mathbf{p}_k(:,i) - \mathbf{m}_{k|k-1}$$

where ν_d is the distribution of the process noise and ζ_{ν_d} is the maximum value achievable by the process noise density.

Using the measurement model the likelihood function $p(\mathbf{z}_k|\mathbf{x}_k)$ can be determined as

$$p(\mathbf{z}_k|\mathbf{x}_k) = \zeta_{\varpi_d} \exp(-(\mathbf{z}_k - \bar{\mathbf{z}}_k)' R_k^{-1}(\mathbf{z}_k - \bar{\mathbf{z}}_k)/2); \tag{39}$$

where the mean of $\mathbf{z}_k$

$$\bar{\mathbf{z}}_k = h(\mathbf{p}_k(:,i), \mathbf{B}_e, \mathbf{S}_k) \tag{40}$$

and ϖ_d is the distribution of measurement noise and ζ_{ϖ_d} is the maximum value achievable by the measurement noise density.

The proposed density is determined as

$$q(\mathbf{x}_k|\mathbf{x}_{k-1}, \mathbf{z}_k) = \zeta_\mu \exp(-(\mathbf{p}_k(:,i))' P_k^{-1}(\mathbf{p}_k(:,i))/2); \tag{41}$$

where ζ_μ is the maximum value achievable by the proposed density.

The weights ω_k are updated as

$$\omega_k(i) = \omega_{k-1}(i) \frac{p(\mathbf{z}_k|\mathbf{x}_k) p(\mathbf{x}_k|\mathbf{x}_{k-1})}{q(\mathbf{x}_k|\mathbf{x}_{k-1}, \mathbf{z}_k)} \tag{42}$$

This recursive process is repeated for all the number of particles. Finally, each element of the weight vector is divided by the sum of the weight vector and the posterior density at scan k can be determined as using (31).

VII. RESULTS

Magnetic anomaly detection (MAD) is a highly nonlinear problem and it has been used in practical applications such as maritime surveillance [3]. MAD normally allowed an aircraft to localize a contact made with sonobuoy. Often in maritime surveillance target of interest is detected and initialized in advance using sonobuoy or other methods. The scenario here is tracking a single target using scalar MAD observations. We present measured results. Note that we have made no attempt to include the $1/f$ (f–frequency) [19] type noise due to geology and geomagnetic activity, but using a white noise level corresponding to roughly 10 pico Tesla/$\sqrt{\text{Hz}}$.

The scenario is considered the general case with 10 dimensions. MAD observation is taken on a specified locations in the Bahamas using a total-field magnetic sensor (magnetometer), mounted in a National Research Council of Canada aircraft. This real scenario is dealt with a single target and the sampling time is $1/32$ sec. The total-field quantity is the scalar total field after all noise reduction processing, including removal of the Earth's core magnetic field as modeled by the 2006 International Geophysical Reference Field (IGRF) based on the latitude, longitude, and altitude of the aircraft. There has been no appreciable filtering applied to process the data. The aircraft altitude data came from GPS and agrees closely with the inertial altitude of the airborne platform. However, both indicated that the plane was 75 ft below sea level when sitting on the runway prior to take off, so we strongly suspect that the actual altitude above water was about aircraft altitude + 75 ft. Observed case is used the Generic Particle filter (GPF), Auxiliary Particle filter (APF), Extended Kalman filter (EKF) and EKF-GPF for tracking.

The tracking problem considered is a real-time single surface target tracking problem and used one exemplar run. To analyse the performance of the filters the performance metrics i.e., Root Mean Square Error (RMSE) and Normalized Estimation Error Squared (NEES) are used. The performance measure is not exceptionally meaningful for multimodal problem, but it has been used in many literature for quantitative comparison [2]. Note, the problem considered is a single model problem. The true states of the target for the exemplar run are known. All the particle filters have 1000 particles and employ resampling at every time step ($N_T = N_s$). The tracking parameters are selected as in Tables (I) and (II).

TABLE I
TRACKING PARAMETERS

Variables	Values
Sampling time (T)	$1/32$ (s)
Number of scans	500
Process noise variance (q)	0.05
Number of particles	1000
Ellipticity	0.00335
Equatorial radius	6378100 (m)

The process noise with zero mean and covariance

$$Q = \begin{bmatrix} T^3/3 & T^2/2 & 0 & 0 & 0 & 0 & 0 & 0 & 0 & 0 \\ T^2/2 & T & 0 & 0 & 0 & 0 & 0 & 0 & 0 & 0 \\ 0 & 0 & T^3/3 & T^2/2 & 0 & 0 & 0 & 0 & 0 & 0 \\ 0 & 0 & T^2/2 & T & 0 & 0 & 0 & 0 & 0 & 0 \\ 0 & 0 & 0 & 0 & 1 & 0 & 0 & 0 & 0 & 0 \\ 0 & 0 & 0 & 0 & 0 & 1 & 0 & 0 & 0 & 0 \\ 0 & 0 & 0 & 0 & 0 & 0 & 1 & 0 & 0 & 0 \\ 0 & 0 & 0 & 0 & 0 & 0 & 0 & 1 & 0 & 0 \\ 0 & 0 & 0 & 0 & 0 & 0 & 0 & 0 & 1 & 0 \\ 0 & 0 & 0 & 0 & 0 & 0 & 0 & 0 & 0 & 1 \end{bmatrix} \quad (43)$$

and the measurement noise with mean zero and covariance $R = 2.5$. The state initial means is selected to be $\mathbf{x}_0 = [0\ 0\ 0\ 0\ 0\ 0\ 0\ 0\ 0\ 0]$ and the initial covariance

$$P_0 = \begin{bmatrix} Rx & 0 & 0 & 0 & 0 & 0 & 0 & 0 & 0 & 0 \\ 0 & \dot{R}x & 0 & 0 & 0 & 0 & 0 & 0 & 0 & 0 \\ 0 & 0 & Ry & 0 & 0 & 0 & 0 & 0 & 0 & 0 \\ 0 & 0 & 0 & \dot{R}y & 0 & 0 & 0 & 0 & 0 & 0 \\ 0 & 0 & 0 & 0 & R & 0 & 0 & 0 & 0 & 0 \\ 0 & 0 & 0 & 0 & 0 & R & 0 & 0 & 0 & 0 \\ 0 & 0 & 0 & 0 & 0 & 0 & R & 0 & 0 & 0 \\ 0 & 0 & 0 & 0 & 0 & 0 & 0 & R & 0 & 0 \\ 0 & 0 & 0 & 0 & 0 & 0 & 0 & 0 & R & 0 \\ 0 & 0 & 0 & 0 & 0 & 0 & 0 & 0 & 0 & R \end{bmatrix} \quad (44)$$

where $R = 2.5$, $Rx = Ry = 1^2$ and $\dot{R}x = \dot{R}y = 0.1^2$.

TABLE II
EARTH'S MAGNETIC INFO AROUND BAHAMAS

Variables	Values (F)
Earth's magnetic field	$[25000\ \ -3400\ 36000] * 10^{-}9$
M_{LP}	$1e+7$
M_{TP}	$1e+6$
M_{VP}	$1e+7$
C_LW	800
C_TW	100
C_VW	1400

The EKF local linearization and Gaussian approximation are not a sufficient of the nonlinear and non-Gaussian nature of the example. Even though the system is a linear, but the measurement equation is a very highly non-linear. As a result during the update recursive the posterior density becomes highly nonlinear and non-Gaussian problem. Which leads the EKF inadequately approximate the posterior density. Unlike the particle filters, EKF performance depends on the selection of initial states. For particle filters, the initial particles are distributed around an area of intrest or can be used in the whole surveillance region. Note, as shown in Figure (1), the detection of the target is confirmed after the field measurement about a certain threshold 1 (nT) and the true values of filed information are known around the surveillance area as in Table (II). Initial state for EKF is selected using the truth, but as shown in Figures (2) – (11) and (17) the mean of the filter is rarely close to the true state. In terms of the NEES from Figure (12) EKF is performed well, but RMSE performance from and Figure (13) indicates as with respect to time the EKF is the least accurate of all the algorithm at approximating the posterior.

The GPF is used the prior distribution as the important density. As shown in Figures (2) – (17) GPF gives good results with thousand number of particles. The RMSE metric shows a marginal improvement over the EKF. To achieve more accurate states, one can simply increase the number of particles, but with the higher complexity. The APF performance can be compared to the GPF and EKF-GPF. Here, proposed particles chosen in more intelligent manner to have a better results e.g., distribute the particles for the whole surveillance area. The APF uses μ_k^i as sample from $p(\mathbf{x}_k|\mathbf{x}_{k-1}^i)$. As shown in Figures (12) and (13) in terms of RMSE and NEES the APF is performed well and RMSE is slightly reduced from the GPF. In terms of NEES both GPF and APF are preformed inconstantly. In order to get a consistent result a combination of EKF and Generic Particle filter (EKF-GPF) is used. In EKF-GPF the EKF is used for each particle to update the mean and covariance. Using calculated mean and covariance a Gaussian distribution is created. From Gaussian distribution samples are drawn. In terms of RMSE all the filters are performed well compared to the PCRLB [25], but as shown in Figure (13) EKF's RMSE metric became poor in time. As shown in Figures (2) – (17) the EKF-GPF is performed well. In terms of NEES it is performed well compared to the rest of the particle filters.

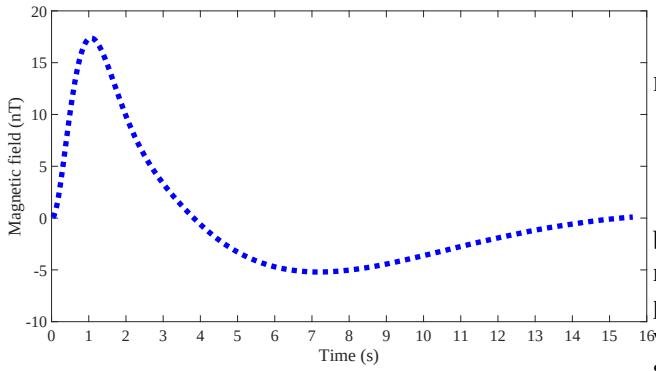

Fig. 1. Magnetic Anomaly

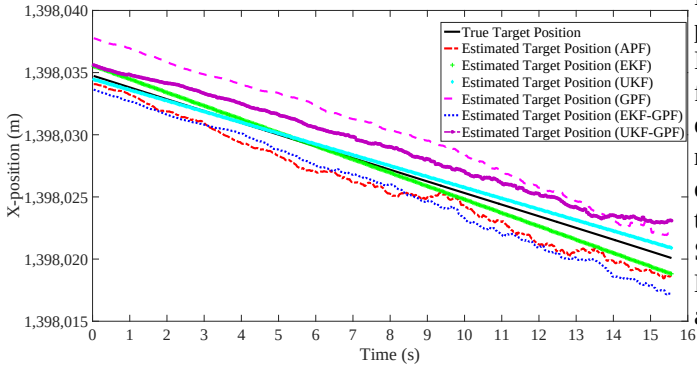

Fig. 2. True X-Position vs. Estimated X-Position

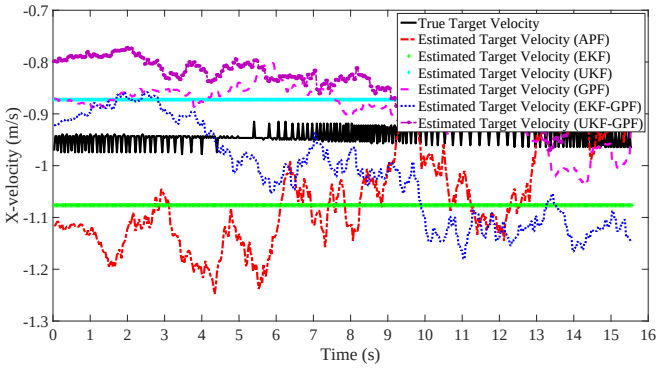

Fig. 3. True X-Velocity vs. Estimated X-Velocity

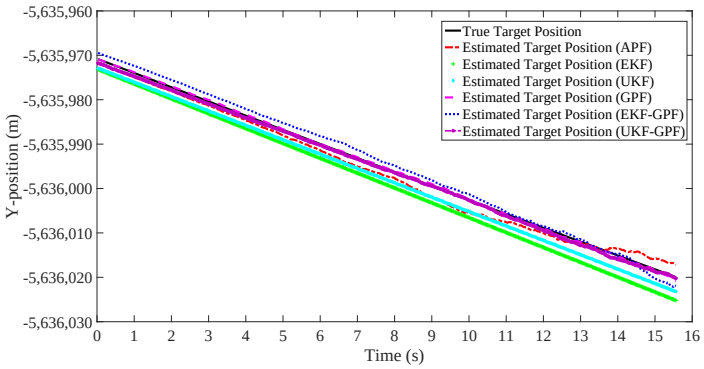

Fig. 4. True Y-Position vs. Estimated Y-Position

VIII. Conclusion

The problem of tracking a vessel modelled at a distance by an equivalent magnetic dipole is investigated. Tracking a magnetic dipole from magnetic filed measurements is a complex non-linear problem. The determination of target position, velocity and magnetic moment is formulated as an optimal stochastic estimation problem, which could be solved using the non-linear filters such as the Extended Kalman filter (EKF), Generic Particle filter (GPF) , Auxiliary Particle filter (APF) and a combination of Extended Kalman filter and Generic Particle filter (EKF-GPF). Obtained results show that the target position, velocity and moment can be accurately determined. It is shown that the particle filters are the best non-linear filter for this application where particle filters are extremely effective at quickly converging on an estimate of the dipole moment of a ship/submarine while minimizing the error in the estimated magnetic field and target position. The results lead to the practicality of including MAD in an airborne Intelligence, Surveillance, Reconnaissance (ISR) architectures. Where the MAD output can be intelligently integrated with that of other airborne sensors such as maritime radar and Cardioid sensor.

Appendix

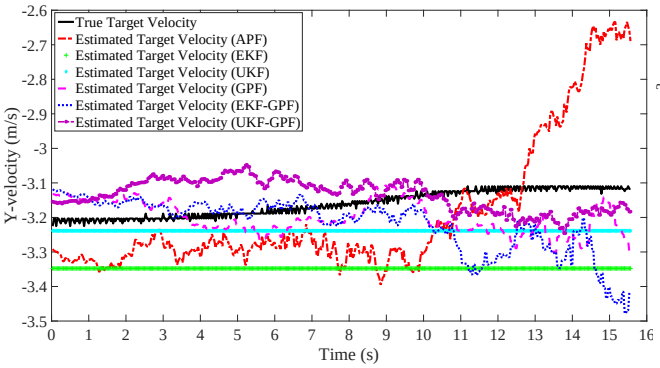

Fig. 5. True Y-Velocity vs. Estimated Y-Velocity

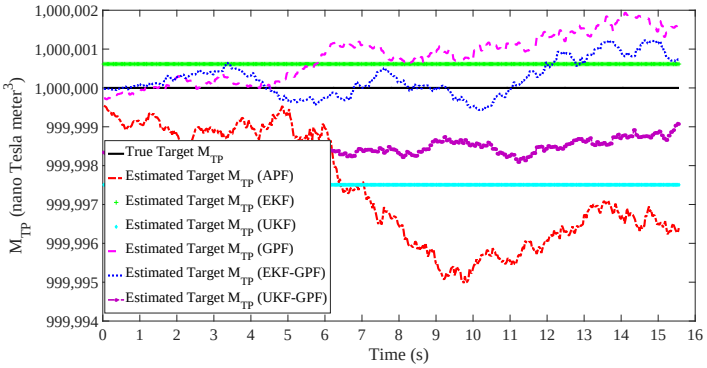

Fig. 7. True MT vs. Estimated MT

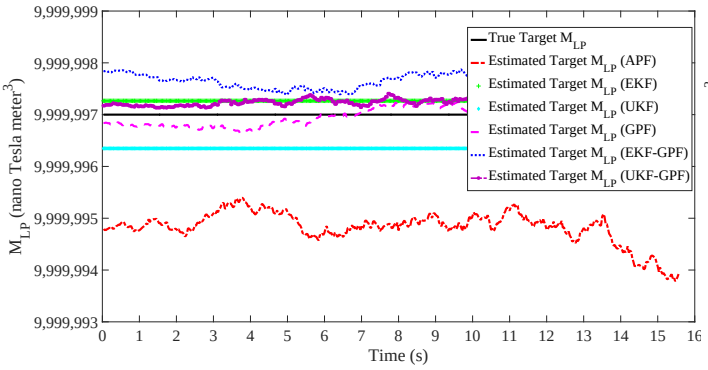

Fig. 6. True ML vs. Estimated ML

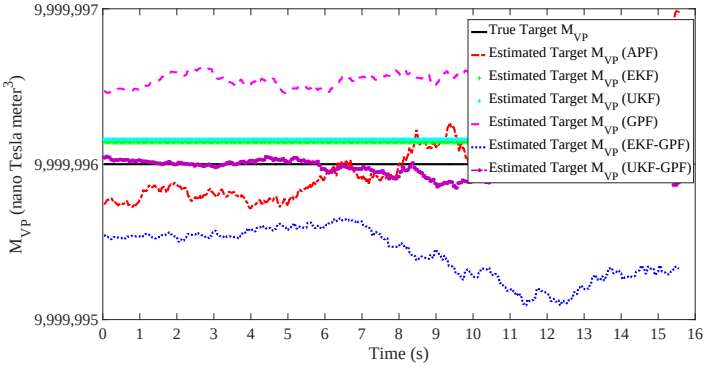

Fig. 8. True MV vs. Estimated MV

REFERENCES

[1] Antepli, M., Gurbuz, S., and Uysal-Biyikoglu, E., "Ferromagnetic target detection and localization with a wireless sensor network", *Proceeding of MILCOM Conference*, pp. 1068–1073, 2010.

[2] Bar-Shalom, Y., Willett, P. K., and Tian, X., *Tracking and Data Fusion*, YBS Publishing, 2011.

[3] Bhashyam, B., and Bradley, J. N., "Parameter estimation and tracking of a magnetic dipole", *Proceeding of SPIE*, vol. 9091, pp. 1–10, June. 2014.

[4] Bradley, J. N., Francois, M., and Edmund, K,. "Target localization from a single MAD pass part 1: Computer simulation", *Defence Research Establishment Atlantic's Technical Memorandum*, pp. 1–18, Mar. 2000.

[5] Bradley, J. N., "Target localization from a single MAD pass part 2: Airborne trials with the AUTEC ROVER", *Defence Research Establishment Atlantic's Technical Memorandum*, pp. 1–14, Apr. 2000.

[6] Birsan, M., "Unscented particle filter for tracking a magnetic dipole target", *MTS/IEEE Transactions on OCEANS*, vol. 2, pp. 1656–1659, 2005.

[7] Birsan, M., "Prediction of the ship's permanent magnetization", *Defence Research Establishment Atlantic's Technical Memorandum*, pp. 1–20, Nov. 2008.

Algorithm 1 Resampling Algorithm

$[\{\mathbf{x}_k^{j*}, \omega_k^{j*}, i^j\}_{j=1}^{N_s}]$ = RESAMPLE$[\{\mathbf{x}_k^i, w_k^i\}_{i=1}^{N_s}]$
Initialize the CDF: $c_1 = 0$
FOR i=1:N_s
– Construct CDF: $c_i = c_{i-1} + \omega_k^i$
END FOR
Start at the bottom of the CDF: i=1
Draw a starting point: $u_1 \backsim \mathbb{U}[0, N_s^{-1}]$
FOR j=1:N_s
– Move along the CDF: $u_j = u_1 + N_s^{-1}(j-1)$
– WHILE $u_j > c_i$
* i = i + 1
– END WHILE
– Assign sample: $\mathbf{x}_k^{j*} = \mathbf{x}_k^i$
– Assign weight: $\omega_k^j = N_s^{-1}$
– Assign parent: $i^j = i$
END FOR

Algorithm 2 Generic Particle Filter

$[\{\mathbf{x}_k^i, \omega_k^i\}_{i=1}^{N_s}]$ = PF$[\{\mathbf{x}_{k-1}^i, w_{k-1}^i\}_{i=1}^{N_s}, \mathbf{z}_k]$
FOR i=1:N_s
– Draw $\mathbf{x}_k^i \sim q(\mathbf{x}_k|\mathbf{x}_{k-1}^i, \mathbf{z}_k)$
– Assign the particle a weight, ω_k^i,
$\omega_k^i \propto \omega_{k-1}^i \frac{p(\mathbf{z}_k|\mathbf{x}_k^i)p(\mathbf{x}_k^i|\mathbf{x}_{k-1}^i)}{q(\mathbf{x}_k^i|\mathbf{x}_{k-1}^i, \mathbf{z}_k)}$
END FOR
Calculate total weight: t = SUM$[\{\omega_k^i\}_{i=1}^{N_s}]$
FOR i=1:N_s
– Normalize: $\omega_k^i = t^{-1}\omega_k^i$
END FOR
Calculate $\hat{N}_{eff} = \frac{1}{\sum_{i=1}^{N_s}(\omega_k^i)^2}$
IF $\hat{N}_{eff} < N_T$
– Resample using algorithm (2):
* $[\{\mathbf{x}_k^i, \omega_k^i, -\}_{i=1}^{N_s}]$ = RESAMPLE$[\{\mathbf{x}_k^i, w_k^i\}_{i=1}^{N_s}]$
END IF

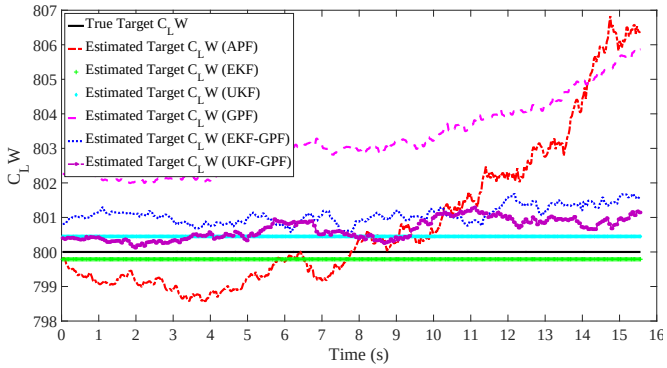

Fig. 9. True CLW vs. Estimated CLW

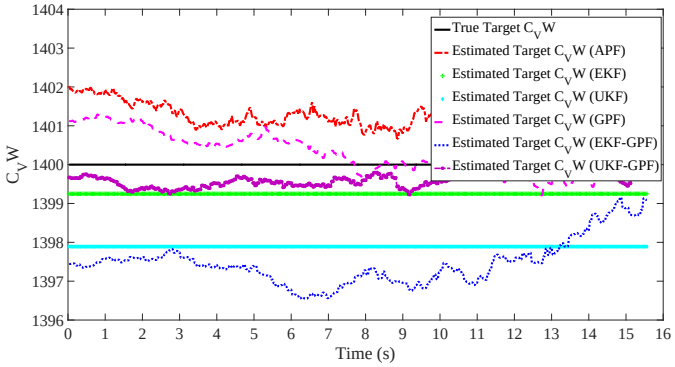

Fig. 11. True CVW vs. Estimated CVW

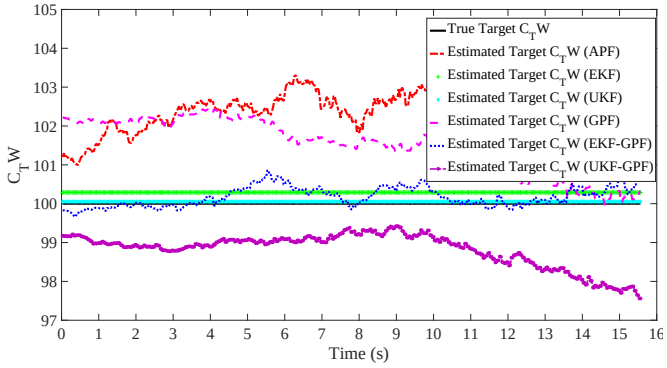

Fig. 10. True CTW vs. Estimated CTW

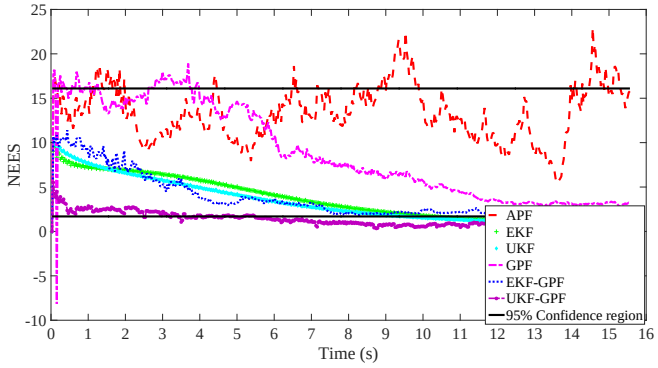

Fig. 12. NEES

[8] Birsan, M., "Recursive bayesian method for magnetic dipole tracking with a tensor gradiometer", *IEEE Transactions on Magnetics*, vol. 47, no. 2, pp. 409–415, Feb. 2011.

[9] Callmer, J., Skoglund, M., and Gustafsson, F., "Silent localization of underwater sensors using magnetometers", *EURASIP Journal on Advances in Signal Processing*, 2010.

[10] Dini, D. H., Mandic, D. P., "An enhanced bearing estimation technique for DIFAR sonobuoy underwater target tracking", *Proceeding of IEEE Conferecne on Sensor Signal Processing for Defence*, pp. 1–4, Sep. 2012.

[11] Doucet, A., De Freitas, N., and Gordon, N., *Sequential Monte Carlo Methods in Practice*, Springer, New York, 2001.

[12] Grewal, M., and Andrews, A., "Applications of kalman filtering in aerospace 1960 to the present", *IEEE Transactions on Control Systems*, vol. 30, no. 3, pp. 69–78, 2010.

[13] Ginzburg, B., Sheinker, A., Frumkis, L., Kaplan, B. Z., and Salomonski, N., "Investigation of advanced data processing technique in magnetic anomaly detection systems", *International Journal on Smart Sensing and Intelligent Systems*, vol. 1, no. 1, pp. 110–122, Mar. 2008.

[14] Hirota, M., Furuse, T., Ebana, K., Kubo, H., Tsushima, K., Inaba, T., Shima, A., Fujinuma, M., and Tojyo, N., "Magnetic detection of a surface ship by an airborne lts squid mad", *IEEE Transactions on Applied Superconductivity*, vol. 11, no. 1, pp. 884–887, Mar. 2001.

[15] Humphrey, K., Horton, T., and Keene, M., "Detection of mobile targets from a moving platform using an actively shielded, adaptively balanced squid gradiometer", *IEEE Transactions on Applied Superconductivity*, vol. 15, no. 2, pp. 753–756, June 2005.

[16] Lenz, J., "A review of magnetic sensors", *Proceedings of the IEEE*, vol. 78, no. 69, pp. 973–989, June 1990.

[17] Lenz, J., and Edelstein, A. S., "Magnetic sensors and their applications", *IEEE Transactions on Sensors Journal*, vol. 6, no. 3, pp. 631–649, June 2006.

[18] Maranda, B. H., "The statistical accuracy of an arctangent bearing estimator", *Proceeding of IEEE Conferecne on Oceans*, vol. 4, pp. 2127–2132, Sep. 2003.

[19] Milotti, E., *1/f noise: a pedagogical review*, ArXiv Physics e-prints, Apr. 2002.

[20] Pei, Y. H., and Yeo, H. G., "Uxo survey using vector magnetic gradiometer on autonomous underwater vehicle", *MTS/IEEE Transactions on OCEANS*, pp. 1–8, 2009.

[21] Peng, D., Chun-sheng, L., Jian, Z., and Bin, T., "Adaptive detection of magnetic target in aeromagnetic survey", *IEEE International Conference on Computer Science and Information Technology*, vol. 2, pp. 497–501, 2010.

[22] Sheinker, A., Ginzburg, B., Salomonski, N., Dickstein, P., Frumkis, L., and Kaplan, B.-Z., "Magnetic anomaly detection using high-order crossing method", *IEEE Transactions on Geoscience and Remote Sensing*, vol. 50, no. 4, pp. 1095–1103, Apr. 2012.

[23] Sheinker, A., Frumkis, L., Ginzburg, B., Salomonski, N., and Kaplan, B.-Z., "Magnetic anomaly detection using a three-axis magnetometer", *IEEE Transactions on Magnetics*, vol. 45, no. 1, pp. 160–167, Jan. 2009.

[24] Schweppe, F., "Evaluation of likelihood functions for gaussian signals", *IEEE Transactions on Information Theory*, vol. 11, no. 1, pp. 61–70, Apr. 1965.

[25] Tharmarasa, R., Kirubarajan, T., Hernandez, M. L., and Sinha, A., "PCRLB based multisensor array management for multitarget tracking", *IEEE Transactions on Aerospace and Electronic Systems*, vol. 43, pp. 539–555, Apr. 2007.

[26] Tang, J.-F., Shi, J.-L., Yang, Y.-H., Heng, H., and Jiang, H.-L., "The solution of target parameter inversion problem based on dipole and scalar magnetometer model", *International Congress on Image and Signal Processing*, vol. 7, pp. 3077–3081, 2010.

[27] Vo, B.-N., Singh, S., and Doucet, A., "Random finite sets and sequential Monte Carlo methods in multi-target tracking", *Proceedings of the international Radar Conference*, pp. 486–491, Sep. 2003.

[28] Wahlstrom, N., Callmer, J., and Gustafsson, F., "Single target tracking using vector magnetometers", *IEEE International Conference on Acoustics, Speech and Signal Processing*, pp. 4332–4335, 2011.

[29] Wahlstrom, N., Callmer, J., and Gustafsson, F., "Magnetometers for tracking metallic targets", *Proceedings of the Information Fusion Conference*, pp. 1–8, 2010.

[30] Yu, H., and ling Hao, Y., "Method of separating dipole magnetic anomaly from geomagnetic field and application in underwater vehicle

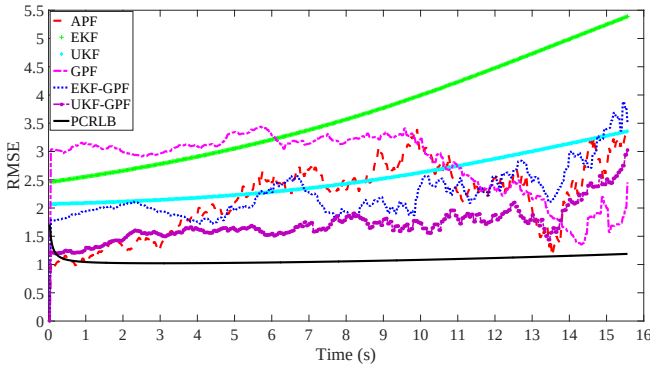

Fig. 13. RMSE

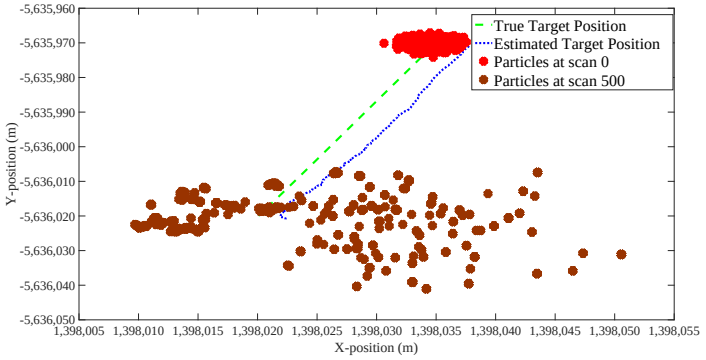

Fig. 15. Auxiliary Particle Filter

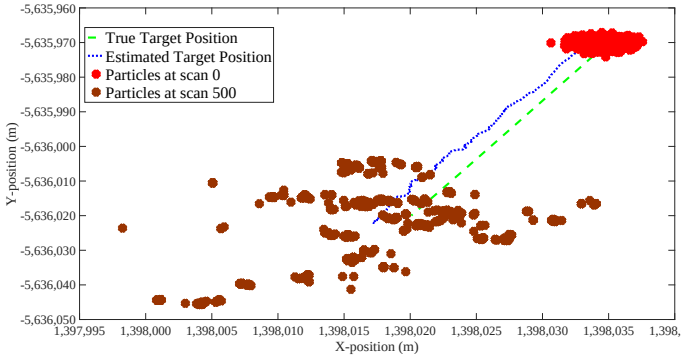

Fig. 14. Generic Particle Filter

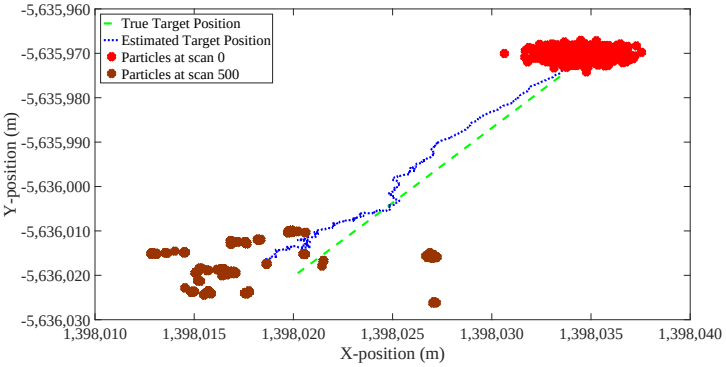

Fig. 16. EKF - Generic Particle Filter

localization", *IEEE International Conference on Information and Automation*, pp. 1357–1362, June 2010.

[31] Zozor, S., Rouve, L.-L., Cauffet, G., Coulomb, J.-L., and Henocq, H., "Compared performances of MF-based and locally optimal-based magnetic anomaly detection", *Proceeding of European Signal Processing Conference*, pp. 149–153, Aug. 2010.

Rajiv Sithiravel received a B.Eng. in Electrical and Computer Engineering from Ryerson University in Toronto, Canada in 2006, M.Eng. degrees in Electrical and Computer Engineering from University of Queensland in Brisbane, Australia in 2007 and from McMaster University in Hamilton, Canada in 2011. PhD degree in Electrical and Computer Engineering from McMaster University, Canada in 2014.

He has been awarded many scholarships including QEII Scholarships in Science and Technology and NSERC's Visiting Fellowship in Canadian Government Laboratories.

From 2008-2009 he was a Consultant in the System Operations Control at Air Canada, Toronto, Canada and he held a post-doctoral position in the Electrical and Computer Engineering department at McMaster University in Hamilton, Canada from 2014 to early 2015. Currently, he has been working as a Defense Scientist in the Radar Sensing and Exploitation division at Department of Research and Development of Canada (DRDC), Ottawa, Canada. At DRDC he has been contributing to numerous airborne sensor based projects including the multisensor data fusion that includes electro-optical (EO) camera, infrared (IR) camera, cardioid sensor, magneto-meter and radar (Synthetic Aperture Radar/Inverse Synthetic Aperture Radar) for Canada's CP-140 program. His research interests include estimation, multitarget tracking, nonlinear filtering, information fusion, signal processing, over the horizon radars, synthetic aperture radar, inverse synthetic aperture radar and magnetic anomaly detection.

Bhashyam Balaji received his B.Sc. (Hons) degree in physics from St. Stephens College, University of Delhi, India and Ph.D. in theoretical particle physics from Boston University, Boston, MA, in 1997.

Since 1998, he has been a scientist at the Defence Research and Development Canada, Ottawa, Canada. His primary research interests include all aspects of radar sensor outputs, including space-time adaptive processing, multitarget tracking, and meta-level tracking including the application of stochastic context-free grammars to syntactic tracking. His theoretical research also includes the application of Feynman path integral and quantum field theory methods to the problems of nonlinear filtering and stochastic control. His recent research includes theoretical and applied aspects of multisource data fusion, including tracking and fusion of sensor outputs from radar, EO/IR, acoustic, electronic support measures, and magnetic anomaly detection sensors.

Ratnasingham Tharmarasa was born in Sri Lanka in 1975. He received the B.Sc.Eng. degree in electronic and telecommunication engineering from University of Moratuwa, Sri Lanka in 2001, and the M.A.Sc and Ph.D. degrees in electrical engineering from McMaster University, Canada in 2003 and 2007, respectively.

From 2001 to 2002 he was an instructor in electronic and telecommunication engineering at the University of Moratuwa, SriLanka. During 2002-2007 he was a graduate student/research assistant in ECE department at the McMaster University, Canada. Currently he is working as a Research Associate in the Electrical and Computer Engineering Department at McMaster University, Canada. His research interests include target tracking, information fusion and sensor resource management.

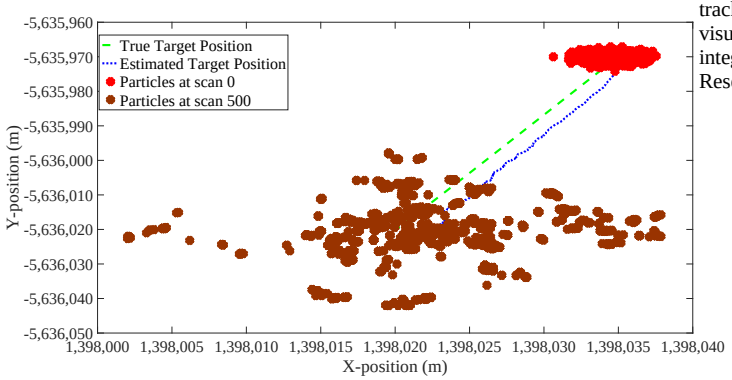

Fig. 17. True Position vs. Estimated Position

Algorithm 3 Auxiliary Particle Filter

$[\{\mathbf{x}_k^i, \omega_k^i\}_{i=1}^{N_s}]$ = APF$[\{\mathbf{x}_{k-1}^i, w_{k-1}^i\}_{i=1}^{N_s}, \mathbf{z}_k]$
FOR $i = 1 : N_s$
– Calculate $\mu_k^i = \mathbb{E}[\mathbf{x}_k|\mathbf{x}_{k-1}^i]$ or a sample $\mu_k^i \sim p(\mathbf{x}_k|\mathbf{x}_{k-1}^i)$
– Calculate $\omega_k^i = q(i|\mathbf{z}_{1:k}) \propto p(\mathbf{z}_k|\mu_k^i)\omega_{k-1}^i$
END FOR
Calculate total weight: $t = \text{SUM}[\{\omega_k^i\}_{i=1}^{N_s}]$
FOR $i = 1 : N_s$
– Normalize: $\omega_k^i = t^{-1}\omega_k^i$
END FOR
Resample using algorithm (2):
– $[\{--, --, i^j\}_{i=1}^{N_s}]$ = RESAMPLE$[\{\mathbf{x}_k^i, w_k^i\}_{i=1}^{N_s}]$
FOR $j = 1 : N_s$
– Draw $\mathbf{x}_k^j \sim q(\mathbf{x}_k|i^j, \mathbf{z}_{1:k}) = p(\mathbf{x}_k|\mathbf{x}_{k-1}^{i^j})$
– Assign weight ω_k^i
$\omega_k^j \propto \omega_{k-1}^{i^j} \frac{p(\mathbf{z}_k|\mathbf{x}_k^j)p(\mathbf{x}_k^j|\mathbf{x}_{k-1}^{i^j})}{q(\mathbf{x}_k^j|\mathbf{x}_{k-1}^{i^j}, \mathbf{z}_k)} = \frac{p(\mathbf{z}_k|\mathbf{x}_k^j)}{p(\mathbf{z}_k|\mu_k^{i^j})}$
END FOR
Calculate total weight: $t = \text{SUM}[\{\omega_k^i\}_{i=1}^{N_s}]$
FOR $i = 1 : N_s$
– Normalize: $\omega_k^i = t^{-1}\omega_k^i$
END FOR

Thiagalingam Kirubarajan (S' 95 M' 98 SM' 03) received the B.A. and M.A. degrees in electrical and information engineering from Cambridge University, England, and the M.S. and Ph.D. degrees in electrical engineering from the University of Connecticut, Storrs. Dr Kirubarajan (Kiruba) holds the title of Distinguished Engineering Professor and holds the Canada Research Chair in Information Fusion at McMaster University, Canada. He has published about 350 research articles, 11 book chapters, one standard textbook on target tracking and four edited volumes. He has lead multiple projects on tracking and fusion with support from the Canadian Department of National Defense, US Air Force, US Navy, NASA, NSERC, Ontario Ministry of Research and Innovation, General Dynamics Canada, Raytheon Canada, ComDev/exactEarth, Toyota, Mine Radio Systems, Qualtech, FLIR Radar Systems and Lockheed Martin Canada. As part of his research at McMaster University, Dr Kirubarajan led the design and development of the distributed multisensor-multitarget tracking testbed for scenario generation, tracking algorithm development and performance evaluation. In addition to conducting research, he has worked extensively with government labs and companies to process real data and to transition his research to the real world. Through his company TrackGen (www.trackgen.com), he has developed a number of software programs, including MultiTrack for real-time large-scale multisensor-multitarget tracking, MultiFuse for distributed tracking, SceneGen for surveillance scenario simulation, and ISR360 for visualization, performance analysis and situation awareness, which have been integrated into many fielded systems. He is a recipient of Ontario Premiers Research Excellence Award and IEEE AESS Barry Carlton Award.